Journal Name

Dynamic Article Links ►

Cite this: DOI: 10.1039/c0xx00000x

www.rsc.org/xxxxxx

ARTICLE TYPE

Easily-prepared dinickel phosphide (Ni_2P) nanoparticles as an efficient and robust electrocatalyst for hydrogen evolution

Ligang Feng,[a] Heron Vrubel,[a] Michaël Bensimon[b] and Xile Hu[a,*]

Received (in XXX, XXX) Xth XXXXXXXXX 20XX, Accepted Xth XXXXXXXXX 20XX

DOI: 10.1039/b000000x

Polydispersed dinickel phosphide (Ni_2P) nanoparticles were synthesized by a simple and scalable solid-state reaction. These nanoparticles are an excellent and robust catalyst for electrochemical hydrogen evolution reaction, operating in both acidic and basic solutions.

The hydrogen evolution reaction (HER) is a reaction of technological significance as it enables the production of hydrogen, a clean energy carrier, from a water-splitting process using electric energy generated from renewable energy sources such as sun and wind.[1] The HER requires a catalyst to take place in a useful rate. Platinum is a highly active catalyst for HER; it has been used in commercial membrane electrolyzers to affect a fast hydrogen production rate while maintaining a high energy efficiency. Platinum is too expensive and rare, however, to be the HER catalyst for the "hydrogen economy", given the scale of global energy demand and the current cost of energy. Instead, a viable catalyst must be made of only Earth-abundant elements. Furthermore, a repertoire of catalysts is warranted in order to meet varying technical specifications for different applications.

Amorphous Ni-P alloys have been studied as HER catalysts since some time, mostly in alkaline solutions.[2, 3] However, these alloys have irregular structure and compositions and their reported activity is conflicting among different samples. In a 2005 DFT study, Liu and Rodriguez predicted that the (001) plane of Ni_2P is a good HER catalyst.[4] In 2013, Schaak, Lewis, and their coworkers experimentally demonstrated the high activity of Ni_2P nanoparticles for HER in acidic solutions.[5] In this pioneering work, hollow and multifacet Ni_2P nanoparticles were prepared by heating nickel(II) acetylacetonate in a solution of 1-octadecene, oleylamine, and tri-n-octylphosphine at 320 °C followed by H_2 treatment at 450°C to remove surface ligands. While this synthesis is sufficient for a first-study, it is corrosive, flammable, and low-yielding. Therefore, alternative and simpler methods to prepare catalytically active Ni_2P nanoparticles are desirable for further structure-activity study of this new catalyst, and for potential applications. Herein, we report that polydispersed Ni_2P nanoparticles prepared by a simple solid phase reaction are an efficient HER catalyst in both acid and basic solutions. These Ni_2P nanoparticles also exhibit a high long-term stability.

Ni_2P nanoparticles were prepared by a thermal reaction of NaH_2PO_2 and $NiCl_2 \cdot 6H_2O$ at 250°C.[6, 7] The freshly prepared samples were passivated in a 1 mol% O_2/N_2 mixture prior to use. Figure 1 shows the X-ray powder diffraction (XRD) pattern for the Ni_2P nanoparticles. Only characteristic peaks corresponding to Ni_2P are observed. The crystal size was calculated to be about 27 nm applying the Scherrer analysis to peak widths.

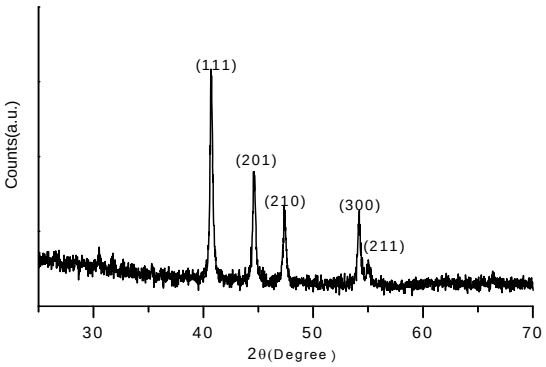

Fig. 1 XRD pattern for Ni_2P nanoparticles

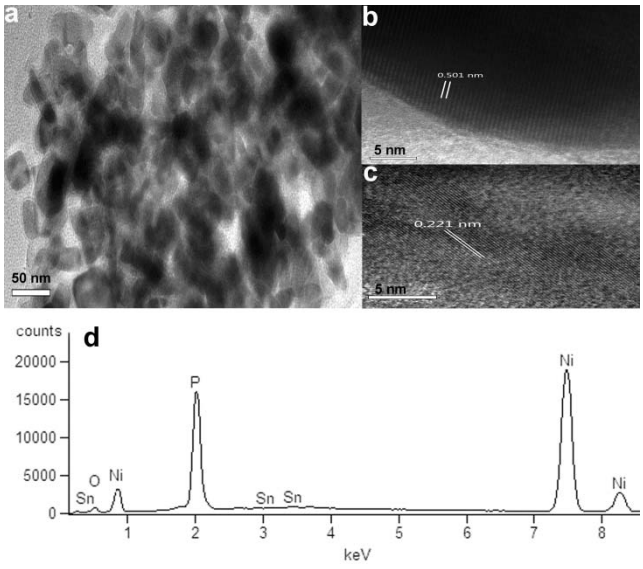

Fig. 2 (a) TEM image of Ni_2P nanoparticles; (b) and (c) HR TEM images of Ni_2P nanoparticles showing different lattice fringes; (d) EDX spectrum of Ni_2P nanoparticles

Transmission Electron Microscopy (TEM) image (Fig. 2, A) shows that the Ni_2P particles are polydispersed nanoparticles of 10-50 nm in diameter. The lattice fringes are visible in the high resolution TEM (Fig. 2, B and C). The distance of 0.221 nm corresponds to the spacing of (111) planes,[8] while that of 0.502 nm corresponds to the spacing of (010) planes.[5] According to energy disperse X-ray (EDX) measurement, the ratio of Ni and P in the bulk sample is close to 2:1(Fig 2, D).

The Ni_2P nanoparticles were drop-casted onto a glassy carbon electrode.† Fig. 3 shows the polarization curve of this modified electrode in 1 M H_2SO_4 (loading: 0.38 mg/cm^2). Catalytic currents could be observed at an overpotential of 50 mV. To produce a current density of 20 mA cm^{-2}, an overpotential of 140 mV is required. The activity of Ni_2P is significantly better than Ni, with an improvement of about 300 mV in overpotential for a same current density. This confirms the ensemble effect provided by P to Ni as predicted by DFT calculations.[4] The activity of these Ni_2P nanoparticles is nearly identical to that of the Ni_2P hollow particles prepared by Schaak, Lewis, and coworkers.[5] This result confirms the intrinsic activity of Ni_2P as a HER catalyst in acidic solutions.

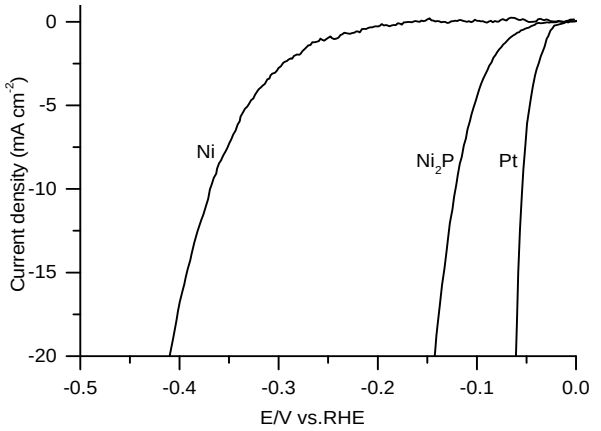

Fig. 3 Polarization curves of an glassy carbon electrode modified with Ni_2P nanoparticles (0.38 mg/cm^2), a Ni electrode, and a Pt electrode in 1 M H_2SO_4; scan rate of 5 mV s^{-1}. The iR drop was corrected.

The activity of Ni_2P particles prepared in this study compares favorably with some of the best non-precious HER catalysts in acidic solutions including molybdenum sulfides, Mo_2C, MoB, NiMoN catalysts (See table S1, ESI for a comparison).†[9-16] All those catalysts require an overpotential of 140 to 240 mV to reach a current density of 10-20 mA cm^{-2}. Pt is still a better catalyst (Fig. 3). However, the lower activity of Ni_2P compared with Pt might be compensated by its lower cost and higher abundance, especially since it can be easily prepared as described here.

The activity of the Ni_2P particles was also investigated in alkaline conditions. Fig. 4 shows the polarization curve of a Ni_2P-modified glassy carbon electrode in 1 M KOH (loading: 0.38 mg/cm^2). The activity is lower than in acid by about 100 mV for a same current density. Catalytic currents are observed at overpotentials larger than 100 mV. To reach a current density of 20 mA cm^{-2}, an overpotential of 250 mV is required. The Ni_2P particles are more active than $Ni(OH)_2$ and Ni under the same conditions, by 50 mV and 80 mV respectively for a same current density (Fig. 4). Ni_2P is less active than Pt, and requires a 100 mV larger overpotential to reach the same current densities (Fig. 4). Overall, the HER activity of Ni_2P in alkaline solutions is comparable to that of Mo_2C and MoB.[17]

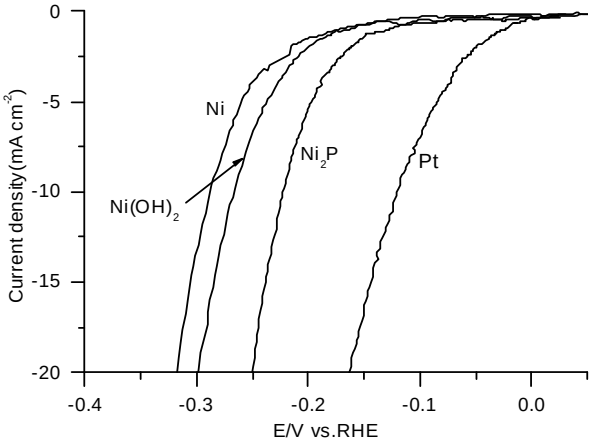

Fig. 4 Polarization curves of a glassy carbon electrode modified with Ni_2P nanoparticles (0.38 mg/cm^2), Ni, $Ni(OH)_2$ (0.4 mg/cm^2), and Pt electrodes in 1 M KOH; scan rate of 5 mV s^{-1}. The iR drop was corrected.

To determine the Faradaic efficiency of HER catalyzed by these Ni_2P particles, the amounts of hydrogen produced during electrolysis at η = 170 mV in 1 M H_2SO_4 and at η = 300 mV in 1 M KOH were measured during 2 hours (Fig. 5). The amount of hydrogen produced matches well with the charge consumed assuming 2 electrons for one H_2. These results indicate a quantitative Faradaic yield for HER catalyzed by Ni_2P in both acid and base solutions.

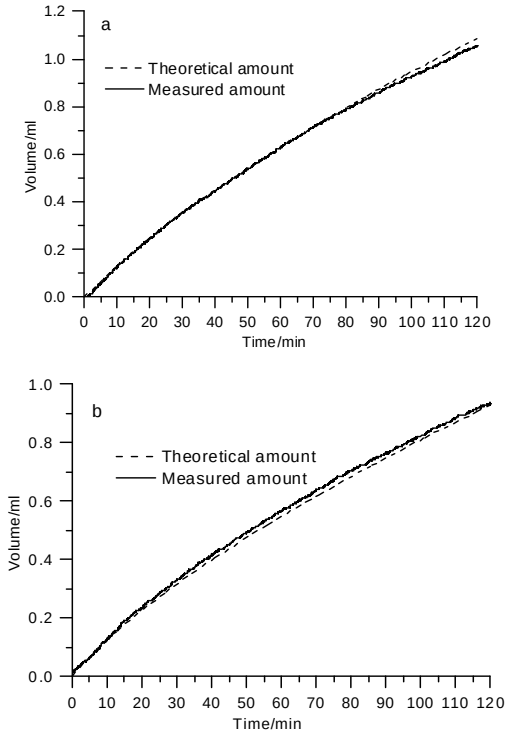

Fig. 5 Current efficiency for HER during potentiostatic electrolysis. A glassy carbon electrode with 0.38 mg/cm^2 Ni_2P was electrolyzed at (a) -170 mV vs. RHE in 1 M H_2SO_4; (b) -300 mV vs. RHE in 1 M KOH. The iR drop was not corrected. The theoretical H_2 lines represent the expected amounts of H_2 assuming a quantitative Faradaic yield. The measured H_2 lines represent the detected H_2.

To test the stability of the Ni_2P nanoparticles under HER conditions, potentiostatic electrolysis was carried out at η = 170

mV in 1M H_2SO_4 and at η = 300 mV in 1 M KOH for 48 hours. In 1 M H_2SO_4, the current was stable at about 20 mA/cm^2 throughout this period (Fig. 6). In 1 M KOH, the current decreased gradually from an initial value of 20 mA cm^{-2}, but remained at about 10 mA cm^{-2} at the end of electrolysis. For comparison, the Ni_2P hollow particles prepared by Schaak, Lewis, and coworkers were partially corroded in acid after 4 hours, and degraded rapidly in base.[5] The polydispersed Ni_2P nanoparticles reported here exhibit improved stability in both acidic and basic solutions. In the current study, Ni_2P was deposited on glassy carbon; in the study of Schaak, Lewis, and coworkers, Ni_2P was deposited on Ti. To check the influence of electrode support on the stability of catalysis, we deposited our Ni_2P particles on a Ti foil. Potentiostatic electrolysis at -150 mV in 1 M H_2SO_4 showed that the current density degraded from 15 mA/cm^2 initially to 5 mA/cm^2 after 10 hours (Fig. S2, ESI). Thus, the lower stability of the Ni_2P-modified electrode observed by Schaak, Lewis, and coworkers is likely due to a poor adhesion of Ni_2P to Ti. To further confirm the stability of Ni_2P particles on glassy carbon during electrolysis, TEM and EDX analysis was made on the particles subject to electrolysis at 13 mA/cm^2 in 1 M H_2SO_4 for 48 h. The morphology and EDX response remained similar to those before electrolysis (Fig. S3, ESI).

Two more experiments were conducted to further probe the stability of Ni_2P. First, an accelerated life-time test was carried out. The electrolysis was maintained at a current density of 140 mA/cm^2, which is more than 10 times higher than the current density expected for a photoelectrochemical device. During 48 h, the initial overpotential was about 300 mV; it remained fairly stable and even decreased to -230 mV in the end (Fig. S4, ESI). This result implies a good stability of Ni_2P under an operating current density of 10 mA/cm^2 or lower (> 600 h). Second, the corrosion of Ni_2P during electrolysis in 1 M H_2SO_4 was monitored using Inductively Coupled Plasma Mass Spectrometry (ICP-MS). To have a good accuracy of measurement, a Ni_2P pellet with a high loading of Ni_2P (250 mg) was fabricated and used as the working electrode. The electrolyte solution was analysed for its Ni content after electrolysis at 10 mA/cm^2 for an interval time. The Ni in the solution might come from corrosion or dissolution of Ni_2P, or from intact Ni_2P particles detached from the electrode during electrolysis. Fig. 7 shows the amount of Ni found in the electrolyte solution, expressed in the percentage of Ni in the original pellet. After 48 h, less than 0.25% of catalyst was removed from the electrode, which again indicated a good long-term stability of Ni_2P. The concentration of Ni in the solution can be fitted with an exponential growth curve, suggesting a first order kinetics for its production (Fig. S5, ESI). Interesting, the fitting indicates that only 500 μg Ni, or 0.25% of Ni_2P can be potentially removed from the electrode. It might be that only a small portion of "special" Ni_2P particles is subject to corrosion or detachment. Alternatively, the appearance of Ni in solution might be a result of dissolution which has equilibrium largely favouring the solid state of Ni_2P. In any case, Ni_2P appears to be stable under catalytic conditions. Although the corrosion rate of Ni_2P is likely dependent of the support materials and the electrode fabrication method, the above results point to a promising long-term stability of Ni_2P.

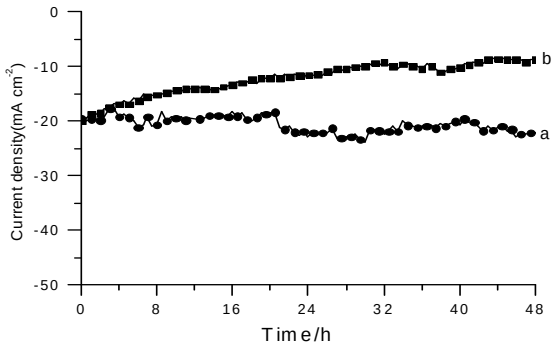

Fig. 6 Time dependence of catalytic currents during electrolysis over 48 hours at (a) -170 mV vs. RHE in 1 M H_2SO_4; (b) -300 mV vs. RHE in 1 M KOH. Loading: 0.38 mg/cm^2. The iR drop was not corrected.

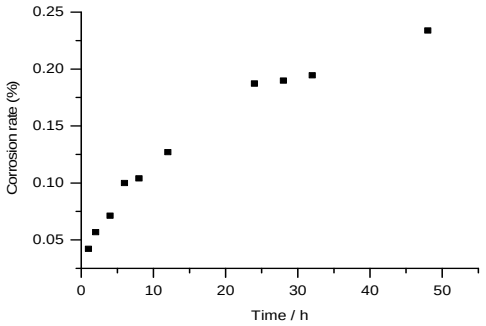

Fig. 7 The rate of corrosion of a Ni_2P electrode during HER electrolysis at 10 mA/cm^2 in 1 M H_2SO_4. The rate is expressed as the percentage of Ni found in the electrolyte.

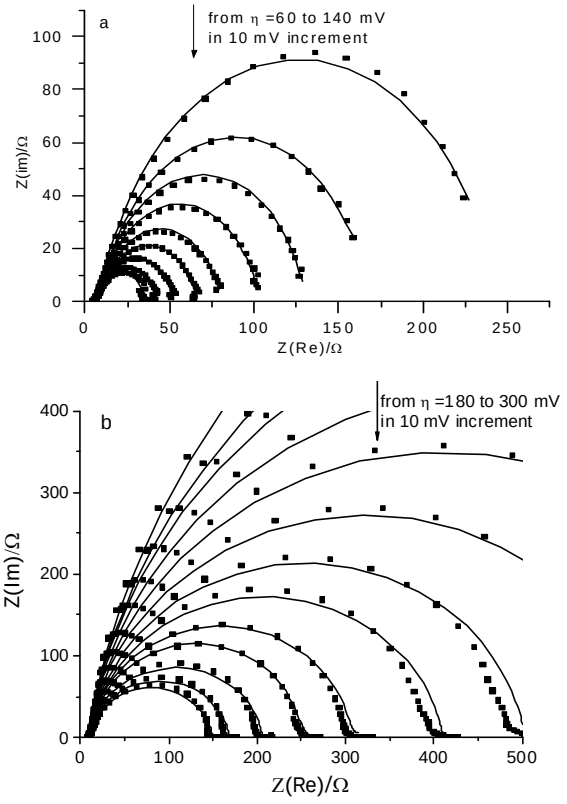

Fig. 8 Nyquist plots of the impedance data for HER catalyzed by a glassy carbon electrode with 0.38 mg/cm^2 Ni_2P (a) in 1 M H_2SO_4 and (b) in 1 M KOH. Squares are the experimental data; solid lines are the fitting.

The electrode kinetics of HER catalyzed by the Ni_2P nanoparticles was studied by impedance spectroscopy. Fig. 8 shows the Niquist plots for the impedance data collected in acidic and alkaline solutions, respectively. The data can be fit using an equivalent circuit (Fig. 9) containing one resistor (R_s) in series with two parallel units of resistor and capacitor. The absence of Warburg impedance excludes the influence of mass transport. The resistance element R_s corresponds to uncompensated solution resistance, while R_1 corresponds to charge transfer resistance arisen from HER. The second time constant (R_2 and CPE_2) is probably related to the contact between the glassy carbon and the catalyst.[18] The plot of $\log(1/R_1)$ vs. η gives the Tafel slope for HER. Thus, a Tafel slope of 87 mV/decade is found for the Ni_2P particles in acid at η >= 60 mV (Fig. 9b); a slope of 100 mV/decade is found in base (Fig. 9c). The Tafel slopes obtained this way reflect better the electrode kinetics than those obtained from the polarization curves, which are 66 mV/decade in acid and 102 mV/decade in base (Fig. S1. ESI). The observed Tafel slopes deviate from a limiting value of 116, 29 or 38 mV/decade predicted assuming a Langmuir isotherm for the adsorption of hydrogen atoms.[19] It has been suggested that intermediate values of Tafel slope arise when the chemisorption of hydrogen requires an activation energy.[20] Hydrogen adsorption may obey Temkin isotherm.[20-22] On the other hand, it is also possible that a Langmuir isotherm applies, but the experimentally determined Tafel slope reflects not only the electrode kinetics, but also the non-uniform distribution of potentials in a porous film.[23]

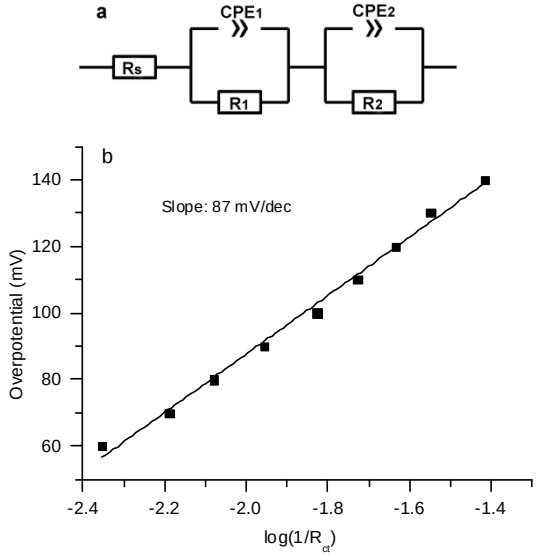

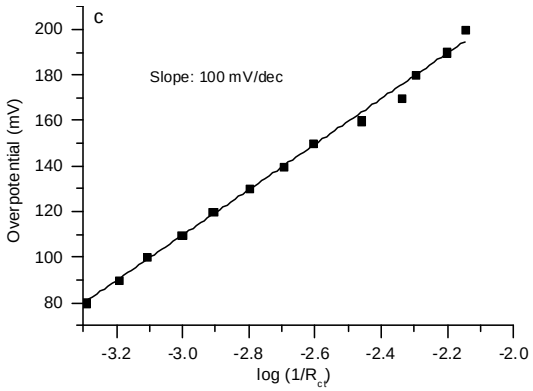

Fig. 9 (a) Electrical equivalent circuit used to model the data from impedance measurements. The plots of overpotential vs. $\log(1/R_1)$ and its linear fitting for data obtained (a) in 1 M H_2SO_4 and (b) in 1 M KOH.

Conclusions

A simple solid-phase reaction of NaH_2PO_2 and $NiCl_2{\bullet}6H_2O$, both inexpensive and abundant reagents, produced Ni_2P nanoparticles that are a highly active catalyst for HER in both acidic and basic solutions. The catalytic activity of this catalyst is one of the highest among non-precious metal catalysts. Compared with earlier reported Ni_2P hollow nanoparticles, the Ni_2P nanoparticles described here are easier and safer to make, and exhibit improved stability. The work is a significant step in the development of Ni_2P as a non-precious HER catalyst for chemical energy storage.

Acknowledgement

This work is supported by a starting grant from the European Research Council (no 257096) and by the CCEM for the Hytech project.

Notes and references

[a]*Laboratory of Inorganic Synthesis and Catalysis, Institute of Chemical Sciences and Engineering, Ecole Polytechnique Fédérale de Lausanne (EPFL), ISIC-LSCI, BCH 3305, Lausanne 1015, Switzerland*
Fax: (+) 49 21 693 9305E-mail: xile.hu@epfl.ch
[b]*General Environmental Laboratory, Institute of Environmental Engineering, Ecole Polytechnique Fédérale de Lausanne (EPFL), Lausanne 1015, Switzerland*
† Electronic Supplementary Information (ESI) available: experimental details, comparison table, and Tafel slopes from polarization curves. See DOI: 10.1039/b000000x/

1. N. S. Lewis and D. G. Nocera, *Proc. Natl. Acad. Sci. USA*, 2006, **103**, 15729-15735.
2. I. Paseka, *Electrochim. Acta* 1995, **40**, 1633-1640.
3. R. K. Shervedani and A. Lasia, *J. Electrochem. Soc.*, 1997, **144**, 511-519.
4. P. Liu and J. A. Rodriguez, *J. Am. Chem. Soc.*, 2005, **127**, 14871-14878.
5. E. J. Popczun, J. R. McKone, C. G. Read, A. J. Biacchi, A. M. Wiltrout, N. S. Lewis and R. E. Schaak, *J. Am. Chem. Soc.*, 2013, **135**, 9267-9270.
6. *This synthesis is a modification of a synthesis described in ref. 7, where NaH_2PO_3 was used as the phosporous souce. NaH_2PO_3 is not commercially available, and was replaced by NaH_2PO_2. As shown in the main text, pure Ni_2P can be prepared using the new method.* .

7. L. M. Song, S. J. Zhang and Q. W. Wei, *Catalysis Communications*, 2011, **12**, 1157-1160.
8. Y. Lu, X. L. Wang, Y. J. Mai, J. Y. Xiang, H. Zhang, L. Li, C. D. Gu, J. P. Tu and S. X. Mao, *J. Phys. Chem. C*, 2012, **116**, 22217-22225.
9. D. Merki and X. L. Hu, *Energy Environ. Sci.*, 2011, **4**, 3878-3888.
10. A. B. Laursen, S. Kegnaes, S. Dahl and I. Chorkendorff, *Energy Environ. Sci.*, 2012, **5**, 5577-5591.
11. Y. G. Li, H. L. Wang, L. M. Xie, Y. Y. Liang, G. S. Hong and H. J. Dai, *J. Am. Chem. Soc.*, 2011, **133**, 7296-7299.
12. D. Merki, S. Fierro, H. Vrubel and X. L. Hu, *Chem. Sci.*, 2011, **2**, 1262-1267.
13. J. Kibsgaard, Z. B. Chen, B. N. Reinecke and T. F. Jaramillo, *Nature Mater.*, 2012, **11**, 963-969.
14. W. F. Chen, K. Sasaki, C. Ma, A. I. Frenkel, N. Marinkovic, J. T. Muckerman, Y. M. Zhu and R. R. Adzic, *Angew. Chem., Int. Ed.*, 2012, **51**, 6131-6135.
15. W. F. Chen, C. H. Wang, K. Sasaki, N. Marinkovic, W. Xu, J. T. Muckerman, Y. Zhu and R. R. Adzic, *Energy Environ. Sci.*, 2013, **6**, 943-951.
16. H. Vrubel and X. L. Hu, *ACS Catal.*, 2013, **3**, 2002-2011.
17. H. Vrubel and X. L. Hu, *Angew. Chem., Int. Ed.*, 2012, **51**, 12703-12706.
18. H. Vrubel, T. Moehl, M. Gratzel and X. L. Hu, *Chem. Commun.*, 2013, **49**, 8985-8987.
19. J. O. M. Bockris and E. C. Potter, *J. Electrochem. Soc.*, 1952, **99**, 169-186.
20. J. G. Thomas, *Trans. Faraday Soc.*, 1961, **57**, 1603-1611.
21. R. Parsons, *Trans. Faraday Soc.*, 1958, **54**, 1053-1063.
22. B. E. Conway and M. Salomon, *Electrochim. Acta* 1964, **9**, 1599-1615.
23. J. N. Soderberg, A. C. Co, A. H. C. Sirk and V. I. Birss, *J. Phys. Chem. B*, 2006, **110**, 10401-10410.